The EMBO Journal (2010) 29, 1637–1651 | © 2010 European Molecular Biology Organization | Some Rights Reserved 0261-4189/10
www.embojournal.org

THE EMBO JOURNAL

EMBO open

Pericentrosomal targeting of Rab6 secretory vesicles by Bicaudal-D-related protein 1 (BICDR-1) regulates neuritogenesis

Max A Schlager[1], Lukas C Kapitein[1], Ilya Grigoriev[2], Grzegorz M Burzynski[3], Phebe S Wulf[1], Nanda Keijzer[1], Esther de Graaff[1,4], Mitsunori Fukuda[5], Iain T Shepherd[3], Anna Akhmanova[2] and Casper C Hoogenraad[1,*]

[1]Department of Neuroscience, Erasmus Medical Center, Rotterdam, The Netherlands, [2]Department of Cell Biology and Genetics, Erasmus Medical Center, Rotterdam, The Netherlands, [3]Department of Biology, Emory University, Atlanta, GA, USA, [4]Department of Clinical Genetics, Erasmus Medical Center, Rotterdam, The Netherlands and [5]Department of Developmental Biology and Neurosciences, Graduate School of Life Sciences, Tohoku University, Sendai, Miyagi, Japan

Membrane and secretory trafficking are essential for proper neuronal development. However, the molecular mechanisms that organize secretory trafficking are poorly understood. Here, we identify Bicaudal-D-related protein 1 (BICDR-1) as an effector of the small GTPase Rab6 and key component of the molecular machinery that controls secretory vesicle transport in developing neurons. BICDR-1 interacts with kinesin motor Kif1C, the dynein/dynactin retrograde motor complex, regulates the pericentrosomal localization of Rab6-positive secretory vesicles and is required for neural development in zebrafish. BICDR-1 expression is high during early neuronal development and strongly declines during neurite outgrowth. In young neurons, BICDR-1 accumulates Rab6 secretory vesicles around the centrosome, restricts anterograde secretory transport and inhibits neuritogenesis. Later during development, BICDR-1 expression is strongly reduced, which permits anterograde secretory transport required for neurite outgrowth. These results indicate an important role for BICDR-1 as temporal regulator of secretory trafficking during the early phase of neuronal differentiation.
The EMBO Journal (2010) **29,** 1637–1651. doi:10.1038/emboj.2010.51; Published online 1 April 2010
Subject Categories: membranes & transport; neuroscience
Keywords: centrosome; dynein motor proteins; neuronal development; Rab GTPase; secretory trafficking

*Corresponding author. Department of Neuroscience, Erasmus Medical Center, Dr Molewaterplein 50, PO Box 2040, Rotterdam 3000CA, The Netherlands. Tel.: +31 0 10 704 3289; Fax: +31 0 10 704 4734; E-mail: c.hoogenraad@erasmusmc.nl

Received: 10 September 2009; accepted: 1 March 2010; published online: 1 April 2010

Introduction

Complex neuronal morphology forms the basis of proper neuronal connectivity and brain function. Establishment of neuronal morphology during development is a highly regulated process in which sprouting and elongation of neurites, later developing into axons and dendrites, is an important event during early neuronal differentiation. Studies in various organisms have provided strong evidence that cytoskeletal changes and membrane trafficking are critical for neurite outgrowth (Bradke and Dotti, 2000; Conde and Caceres, 2009) and that directional trafficking through the secretory pathway is needed to control neurite elongation (Bonifacino and Glick, 2004; Pfenninger, 2009). Secretory- and plasma membrane proteins are collected into secretory vesicles at the *trans*-Golgi network and targeted with molecular motors into growing neurites. Fusion with the plasma membrane permits the secretion of the vesicle contents, as well as the incorporation of vesicular lipids and proteins in neurites. However, it remains unclear how secretory trafficking is coordinated during neuronal differentiation.

The delivery of secretory cargo into neurites primarily depends on the microtubule transport machinery (Zakharenko and Popov, 1998; Erez *et al*, 2007). Vesicles are actively transported along microtubules towards their target membrane by kinesin and dynein motors (Hirokawa and Takemura, 2005). Some motor proteins can directly interact with the membrane surface, but, more typically, cargos interact with motors through intermediate components and/or adaptor proteins including scaffolding and transmembrane proteins (Hirokawa and Noda, 2008; Kardon and Vale, 2009; Schlager and Hoogenraad, 2009). For example, a recently identified adaptor complex containing Milton and Miro participates in binding kinesin-1 to the mitochondrial membranes (Macaskill *et al*, 2009; Wang and Schwarz, 2009). Motor–cargo adaptors not only regulate binding affinities, but also mediate transport specificity and cargo identity, thereby contributing to the regulated delivery of particular cargo to its specific cellular destination (Schlager and Hoogenraad, 2009).

A number of genetic and biochemical studies have implicated Rab GTPases as regulators of specific vesicular traffic pathways (Zerial and McBride, 2001; Stenmark, 2009). Each organelle or vesicle carries its own set of Rabs, which ensures the specificity of intracellular membrane transport. By acting as molecular switches in response to GTP, Rab proteins bind to their effectors, which confer specificity to different membrane compartments (Fukuda, 2008). A number of Rab effector proteins were identified that bind motor proteins and control their recruitment to the specific target membranes (Caviston and Holzbaur, 2006). However, how Rab

proteins and their effectors control vesicular trafficking is poorly understood.

Recently, the small GTPase Rab6A was found to localize to secretory (exocytotic) vesicles in fibroblast cells and have an important function in controlling transport and fusion of these vesicles with the plasma membrane (Grigoriev *et al*, 2007). Among the members of the Rab6 family, Rab6A and Rab6A' are ubiquitously expressed (Echard *et al*, 2000), whereas Rab6B is predominantly present in brain tissue (Wanschers *et al*, 2007). The Rab6 effector protein Bicaudal-D (BICD) participates in recruiting dynein motors to Rab6-carrying vesicles and in their microtubule minus-end-directed transport (Matanis *et al*, 2002; Grigoriev *et al*, 2007). BICD seems to be part of evolutionarily conserved transport machinery; *Drosophila* BicD also associates with Rab6 (Coutelis and Ephrussi, 2007; Januschke *et al*, 2007) and the dynein motor complex (Swan *et al*, 1999). In fly, BicD is crucial for the development of the oocyte and embryo (Claussen and Suter, 2005), facilitates dynein-mediated transport and is involved in the proper localization of mRNA (Bullock and Ish-Horowicz, 2001; Navarro *et al*, 2004). In mammals, two homologues of Bicaudal-D are present, BICD1 and BICD2. The N-terminal part of BICD binds to cytoplasmic dynein and its accessory and regulatory factor dynactin (Hoogenraad *et al*, 2001) and is sufficient to recruit these complexes to organelles (Hoogenraad *et al*, 2003), whereas the C-terminal part of BICD contains the cargo-binding domain and interacts with Rab6 (Matanis *et al*, 2002; Januschke *et al*, 2007).

Here, we searched for proteins with sequences homologous to BICD and identified BICD-related protein 1 (BICDR-1) as a novel effector of Rab6 and component of secretory vesicle machinery in developing neurons. We show that BICDR-1 interacts with the dynein/dynactin motor complex, binds to kinesin-3 motor protein Kif1C and controls the pericentrosomal localization of Rab6-positive secretory vesicles. Sustained expression of BICDR-1 as well as knockdown of Rab6 suppress neurite outgrowth. These results highlight the importance of Rab6 during neuritogenesis and describe a new mechanism for regulating secretory trafficking; BICDR-1 accumulates Rab6 secretory vesicles in the cell body around the centrosome and restricts delivery of these carriers to the neurites during the early phase of neuronal differentiation.

Results

BICDR-1 concentrates around the centrosome and is expressed in kidney and brain

In a sequence homology search for new mammalian BICD-like proteins, we found two previously uncharacterized BICD homologues: hypothetical coiled-coil domain containing protein 64 (Ccdc64) and 64B (Ccdc64B). We renamed these proteins BICDR-1 and BICD-related protein 2 (BICDR-2), respectively. BICDR-1 and BICDR-2 genes are conserved in vertebrates, whereas BICDR-1 is also present in flies (Supplementary Figure S1A and B). In contrast to the three coiled-coil segments in BICD, BICDR proteins are shorter and only contain two predicted coiled-coil regions (Figure 1A). The highest degree of similarity to BICD is found in the cargo-binding domain at the C-terminus of BICDR (64% similarity; Supplementary Figure S1C). Northern blot analysis showed that BICDR-1 is predominantly expressed in kidney and brain, whereas some expression can be seen in testis and heart (Figure 1B). In contrast, BICDR-2 could not be detected on northern blots or tissue dot blots (data not shown). Indeed, expressed sequence tag profiles show that the BICDR-2 gene is expressed at low levels and only detected in a few tissues such as stomach, oesophagus and ovary. In this study, we decided to focus on BICDR-1 and generated rabbit polyclonal antibodies against both the N-terminal (#12) and central (#13) region of the protein (Figure 1A). Both antibodies reacted only to BICDR-1, and not to control proteins BICD1, BICD2 or BICDR-2 (Figure 1C). In agreement with mRNA expression data, western blot analysis of various adult mouse tissues showed that BICDR-1 expression is high in kidney and moderate in testis and brain (Figure 1D).

Next, we examined BICDR-1 expression during mouse development from early embryonic stage (E10.5) to postnatal day 1 (P1). Immunoblots show that BICDR-1 levels are high at early embryonic stages and decrease during embryonic development whereas levels of other markers remained constant (Rab6A, $p150^{glued}$, BICD2, actin) or increased (Rab6B) (Figure 1E). Whole-mount *in situ* hybridization on E9–11 mouse embryos showed BICDR-1 expression throughout the developing brain, in the developing eye and dorsal root ganglia (Figure 1F–H; data not shown). To study the distribution of BICDR-1 in more detail we performed *in situ* hybridization on transverse 10 μm cryosections of E13.5 mouse embryos. Consistently, we found that BICDR-1 is present in the developing kidney (Figure 1I–L) and throughout the developing nervous tissue including the neural layer of the retina (Figure 1M–R) and the dorsal root ganglia (data not shown), whereas the sense control probe showed no labelling (Figure 1M, O and Q). These data indicate that BICDR-1 expression is highest during early embryonic development and predominantly present in kidney, undifferentiated neural tissue and developing eye.

BICDR-1 regulates early neural development in zebrafish

To gain more insight into the functional significance of BICDR-1 during embryonic development, we turned to zebrafish as a vertebrate model system. First, we analysed the distribution of the zebrafish homologue of BICDR-1, zBICDR-1, by whole-mount *in situ* hybridization. Interestingly, the distribution in developing fish embryos closely resembled the distribution found in mouse; restricted expression in developing neural tissue and eye (Figure 2A). Next, two zBICDR-1-specific morpholinos (MOs) were used to block zBICDR-1 expression in zebrafish embryos. Subsequent analysis of the zBICDR-1-MO-treated embryos showed a striking phenotype in which neural development was disrupted and the eye failed to develop, whereas the control, mismatch zBICDR-1-mis-MO, did not show any abnormalities (Figure 2B). To determine the cause of the observed phenotype we stained wild type and zBICDR-1-MO-treated fish with the mitotic marker phospho-H3 and apoptosis markers caspase and acridine orange. Although no differences in phospho-H3 staining were observed, both caspase and acridine orange levels were increased in zBICDR-1-MO fish (Figure 2C), suggesting that the observed developmental defects are most likely explained by an increased neuronal death. Overall these data indicate that zBICDR-1 regulates early neuronal development and survival in zebrafish.

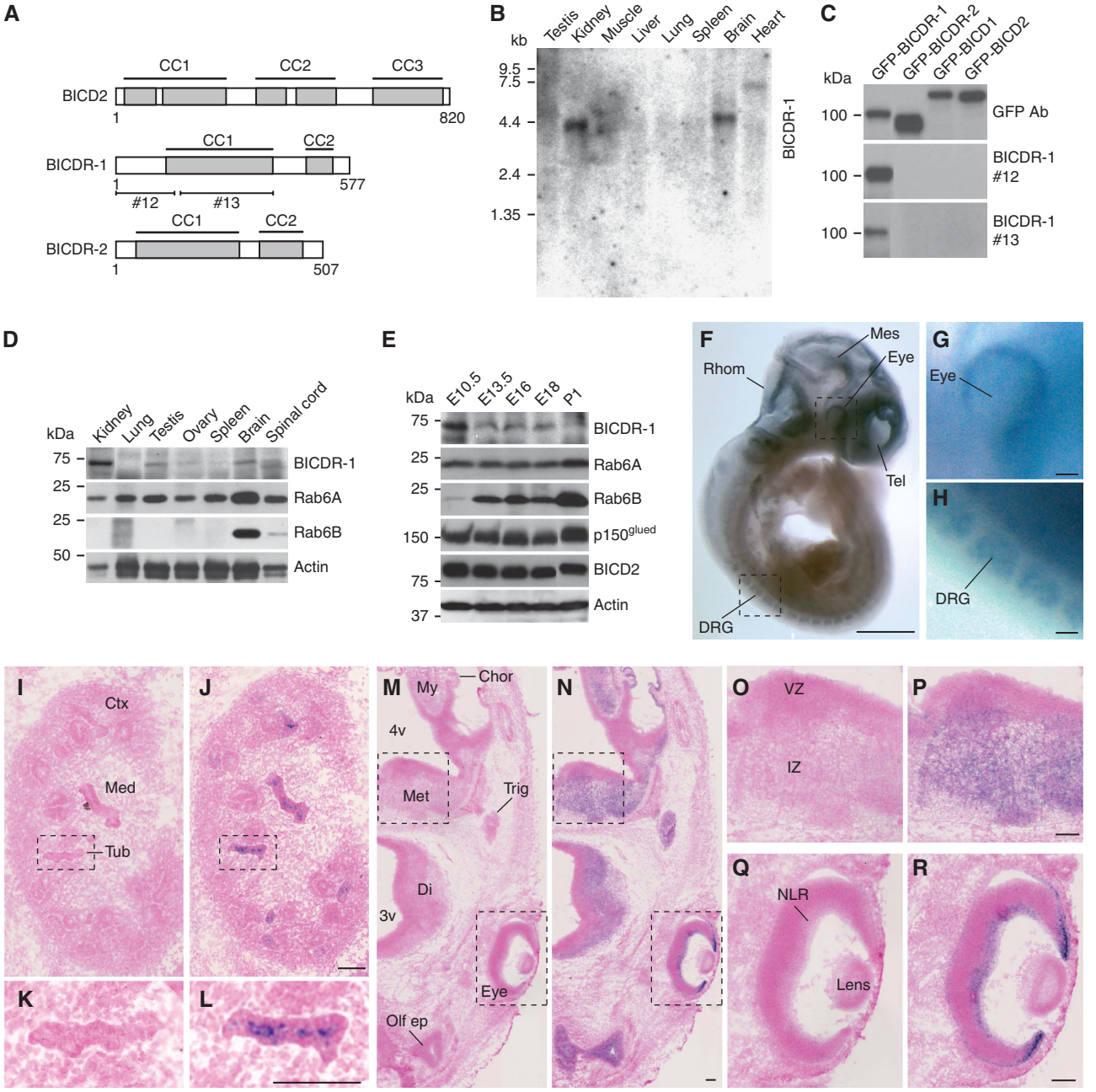

Figure 1 BICDR-1 is mainly expressed in kidney and neural tissues during development. (**A**) Schematic structure of BICD2 and BICDR proteins (CC, coiled-coil region). Antibodies were raised against GST-tagged BICDR-1 fusion proteins containing amino acids 1–146 (antibody #12) and 161–387 (antibody #13). (**B**) Expression of BICDR-1 mRNA in various rat tissues. (**C**) BICDR-1 antibodies #12 and #13 specifically recognize GFP-tagged BICDR-1 not the homologous proteins BICDR-2, BICD1 or BICD2. (**D**) Western blot analysis of BICDR-1, Rab6A and Rab6B in various mouse tissues. (**E**) Developmental expression patterns of BICDR-1, Rab6A, Rab6B, p150^{glued} and BICD2 in E10.5 (whole embryo), E13.5, E16, E18 and P1 (head only) mouse. (**F**–**H**) Lateral view of E10 mouse embryo hybridized with a BICDR-1-specific ribo-probe. Indicated structures: dorsal root ganglion (DRG); mesencephalon (Mes); rhombencephalon (Rhom); telencephalon (Tel). Scale bar in (**F**) 1 mm in (**G**–**H**) 100 μm. (**I**–**L**) Transverse cryosections (10 μm) of an E13.5 mouse kidney, hybridized with a BICDR-1 sense (**I**, **K**) or anti-sense (**J**, **L**) ribo-probe. Indicated structures: cortical region of metanephros (Ctx); medullary region of metanephros (Med); and metanephric tubule (Tub). Scale bars, 100 μm. (**M**–**R**) Transverse cryosections (10 μm) of an E13.5 mouse head, hybridized with a BICDR-1 sense (**M**, **O**, **Q**) or anti-sense (**N**, **P**, **R**) ribo-probe. Indicated structures: fourth ventricle (4v); third ventricle (3v); choroid plexus (Chor); myencephalon (My); metencephalon (Met); diencephalon (Di); trigeminal (V) ganglion (Trig); olfactory epithelium (Olf ep); ventricular zone (VZ); intermediate zone (IZ); neural layer of retina (NLR). Scale bars, 100 μm.

BICDR-1 is a Rab6-binding protein

We next wanted to understand the cellular pathway in which BICDR-1 is involved. Previous studies have shown that members of BICD family interact with the small GTPase Rab6 (Matanis *et al*, 2002; Grigoriev *et al*, 2007). Therefore, we searched for possible interactions of BICDR-1 with Rab-GTPases by glutathione *S*-transferase (GST) pull-down assays with cell lysates expressing FLAG-tagged BICDR-1 using 60

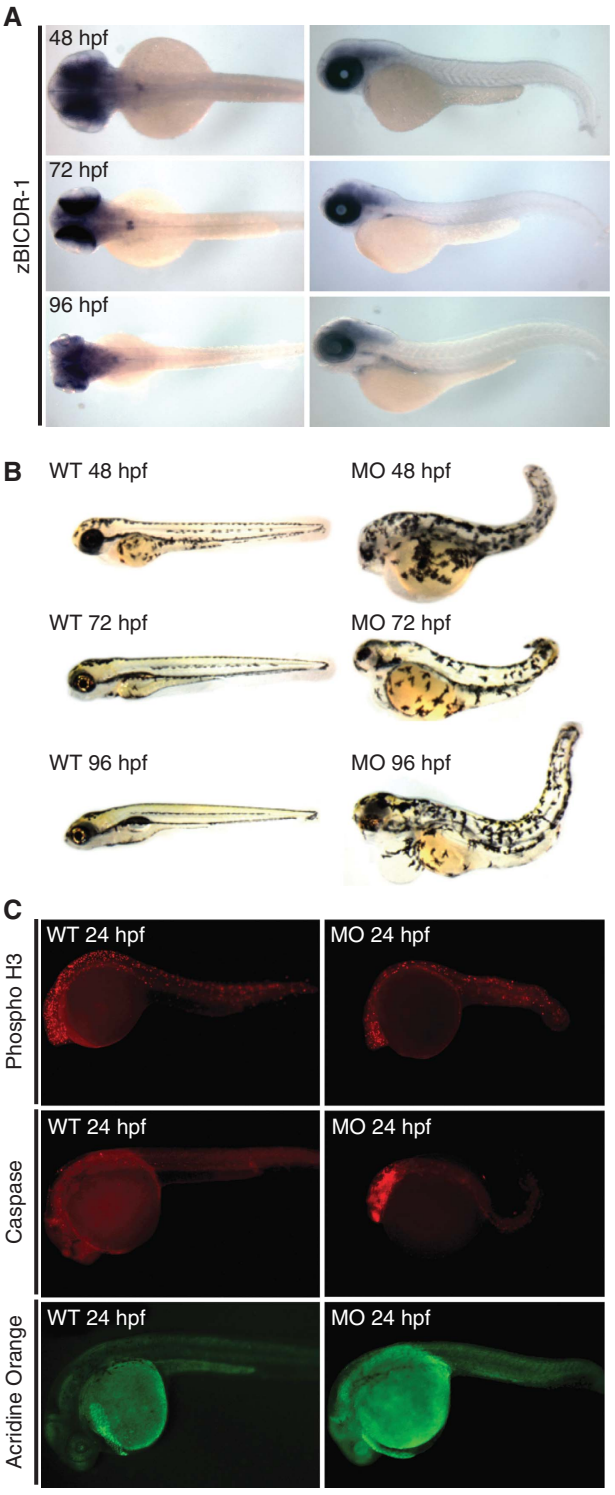

Figure 2 BICDR-1 has a critical role in zebrafish neural and eye development. (**A**) Dorsal and lateral views of zebrafish fixed and *in situ* hybridized with zBICDR-1-specific probe at 48, 72 or 96 hpf. (**B**) Lateral views of wild type (WT) and zBICDR-1 morphant fish (MO) at 48, 72 or 96 hpf. (**C**) Lateral views of wild type (WT) and morphant fish (MO) labelled with phospho-H3 or caspase-specific antibodies or acridine orange.

different recombinant Rab proteins (including 43 subfamilies) immobilized on GST beads. BICDR-1 strongly interacts with only one Rab subfamily, Rab6A/B (Figure 3A, square) and marginally with Rab11B and Rab12, but not with any of the other Rabs tested (Figure 3A). In contrast, BICDR-2 interacts most strongly with Rab13 (Figure 3A). Moreover, both full-length BICDR-1 and a C-terminal region of BICDR-1, amino acids 382–577, interact with constitutively active GTPase-deficient Rab6A-Q72R and not with GDP-locked inactive Rab6A-T27N in the yeast two-hybrid assay (Figure 3B; Supplementary Figure S2A). Binding of BICDR-1 to Rab6A is direct because the purified His-tagged C-terminus of BICDR-1 (amino acids 382–577) interacts with purified GST-Rab6A and GST-Rab6B and not with GST only (Figure 3C). Interestingly, BICDR-1 binds most strongly to the neuron-specific isoform Rab6B (Figure 3A and C). The Rab6-binding region of BICD is well conserved in the C-terminal domain of BICDR-1 and contains a lysine residue (Figure 3E, asterisk) that is mutated to methionine in a loss of function *Drosophila* BicD allele (Ran *et al*, 1994). We next tested whether this mutation would disrupt Rab6 binding. GST-Rab6 pull-down assays with lysates of cells expressing mutant BICDR-1-K512M and an *in vitro* binding assay using purified His-BICDR-1C-K512M showed that lysine 512 is required for binding to Rab6 (Figure 3C). Similarly, BICD2-K785M could not be precipitated by GST-Rab6 (Figure 3D). Moreover, BICDR-1 and BICD2 compete for Rab6 binding in *in vitro* pull-down assays (Supplementary Figure S2B). Together these data show that the conserved C-terminal domain of BICDR-1 directly binds to Rab6A and Rab6B.

BICDR-1 is required for the pericentrosomal localization of Rab6A-positive vesicles

To examine the subcellular distribution of endogenous BICDR-1 we used kidney-derived Vero cells. Fluorescence microscopic analysis showed an intense perinuclear BICDR-1 staining (Supplementary Figure S2C–E) specifically localized around the γ-tubulin-labelled centrosome (Figure 3F). Consistently, the BICDR-1 punctate labelling is concentrated in the centre of the radial microtubule array (Supplementary Figure S2G) but shows no association with the actin cytoskeleton (Supplementary Figure S2H). Both microtubule depolymerization by nocodazole and knockdown of γ-tubulin disrupt the pericentrosomal localization of BICDR-1, whereas actin depolymerization by cytochalasin D has no effect (Supplementary Figure S3A and C). These data suggest that the pericentrosomal BICDR-1 localization is microtubule and γ-tubulin dependent.

Immunofluorescent staining of BICDR-1 and Rab6 showed extensive co-localization around the centrosome, however no co-distribution was observed on Rab6A-positive Golgi stacks (Figure 3G; Supplementary Figure S2F) or with any other Golgi or endosomal markers, such as GM130, γ-adaptin, TGN46, galactosyl transferase and EEA1 (data not shown). To test whether BICDR-1 localization depends on Rab6, Vero cells were transfected with Rab6A-siRNA. In the absence of Rab6A, BICDR-1 was no longer detected at the pericentrosomal region (Supplementary Figure S3D), whereas the localization of other Golgi and endosomal proteins was unaffected (data not shown). BICDR-1 expression levels were unaltered in Rab6 knockdown cells (Supplementary Figure S3B). We next tested whether the specific pericentrosomal localization of Rab6A in Vero cells depends on BICDR-1. Vero cells transfected with three independent BICDR-1-siRNAs (Supplementary Figure S4A–C) clearly showed that, in the absence of BICDR-1, Rab6-positive vesicles no longer cluster

around the centrosomal region, whereas Rab6 staining at the Golgi was unaffected (Supplementary Figure S4D and E). Importantly, the effect of BICDR-1 knockdown on Rab6 transport is not because of alterations in Rab6 expression levels (Supplementary Figure S4A), dynein/dynactin localization (Supplementary Figure S5A) or defects in microtubule organization, because no changes in microtubule nucleation and dynamics were observed (Supplementary Figure S4F). Together these data indicate that BICDR-1 localizes to Rab6-positive vesicles and required for the pericentrosomal distribution of Rab6 vesicles.

BICDR-1 interacts with the dynein/dynactin motor complex

Earlier studies have shown that members of BICD family interact with the microtubule minus-end-directed dynein/dynactin motor complex. Therefore, we investigated the possible interaction between BICDR-1 and dynein/dynactin. Co-immunoprecipitation experiments from Hela cells transfected with GFP-BICDR-1 showed that BICDR-1 precipitates the major dynein/dynactin subunits, whereas no binding is seen with control GFP (Figure 4A). Consistently, both dynactin (Figure 4D) and dynein (Supplementary Figure S5B) co-localize with endogenous BICDR-1 around the centrosome in Vero cells. Overexpression of GFP-BICDR-1 caused an approximately two-fold increase in pericentrosomal dynein/dynactin fluorescent staining intensity (Figure 4B and E; Supplementary Figure S5C), indicating that BICDR-1 recruits the dynein/dynactin motor complex to the pericentrosomal region.

Next, we tested whether the pericentrosomal localization of BICDR-1 depends on dynein/dynactin function. Immunofluorescent staining for endogenous BICDR-1 showed that cells with reduced levels of dynein heavy chain (DHC) or $p150^{glued}$ have lost most of the pericentrosomal BICDR-1 staining (Figure 4F;data not shown). Quantification showed that only ~15% of the dynein/dynactin knockdown cells showed BICDR-1 around the centrosome compared with ~74% in control cells (Figure 4C). Together these data indicate that BICDR-1 interacts with the dynein/dynactin complex and the pericentrosomal distribution of BICDR-1 critically depends on dynein/dynactin function.

BICDR-1 expression strongly declines during neuronal development

Considering the early neuronal BICDR-1 phenotypes in zebrafish, we set out to investigate the possible role for BICDR-1 in neuronal differentiation using primary cultured hippocampal neurons as a model system. First, we analysed the expression of endogenous BICDR-1 during hippocampal neuron development from *in vitro* days 1 to 26 (DIV1–26). Western blot analysis showed that BICDR-1 is highly expressed in undifferentiated neurons at early developmental stages (DIV1) and markedly decreased at later stages (>DIV3) (Figure 5A), similar to what is seen during early embryonic mouse development (Figure 1E). Levels of the BICDR-1-interacting proteins, Rab6A/B and dynactin ($p150^{glued}$), remained constant or increased over time (Figure 5A). Next, we performed immunofluorescent staining of different stages of developing hippocampal neurons with BICDR-1 antibodies. In DIV1–2 neurons, an intense vesicle-like pericentrosomal BICDR-1 staining was observed, whereas a weak vesicular staining was present in some processes (Figure 5B and C). In older neurons (>DIV3), BICDR-1 immunoreactivity was almost undetectable (Figure 5B). A similar decrease in BICDR expression was also observed in developing DRG neurons (data not shown). These data show that BICDR-1 is predominately expressed in early developing neurons before the stage of neurite outgrowth and elongation.

BICDR-1 controls the trafficking of secretory vesicles in neurons

Consistent with the data in Vero cells, endogenous BICDR-1 coincided with a subset of Rab6-positive vesicles in the cell body and dendrites in young neurons (Figure 5C). The ability of BICDR-1 to associate with Rab6 vesicles in neurons was confirmed by simultaneous dual colour live imaging of GFP-Rab6A and mCherry-BICDR-1. BICDR-1 was observed on mobile Rab6-positive secretory vesicles and tubular structures, which docked and fused with larger BICDR-1/Rab6 membrane domains in the cell body (Figure 5D; Supplementary Movie S1). Most mobile secretory vesicles showed both anterograde and retrograde movement in neurites, suggesting that both microtubule plus-end- and minus-end-directed motors are attached to Rab6 secretory vesicles in neurons. We previously showed that Rab6-positive vesicles in Hela cells contain secretory protein markers, such as neuropeptide Y (NPY) and brain-derived neurotrophic factor (BDNF) and showed persistent flow from the Golgi complex to the cell periphery where fusion with the plasma membrane occurs (Grigoriev *et al*, 2007). By using total internal reflection fluorescence microscopy, we could readily visualize the exocytosis of NPY-GFP-labelled vesicles in the cell periphery (Supplementary Movie S2). Hela cells co-transfected with mCherry-BICDR-1 and NPY-GFP and stained for endogenous Rab6A showed that most of the centrosomal BICDR-1-positive vesicles contain NPY-GFP (Supplementary Figure S6A), indicating that both Rab6 and BICDR-1 are present on NPY-labelled secretory carriers. Interestingly, at low level BICDR-1 expression, several Rab6/BICDR-1/NPY vesicles are observed in the cytoplasm and only the minority of the vesicles concentrate around the centrosome (Supplementary Figure S6A). In contrast, adding increasing amounts of BICDR-1 caused pericentrosomal accumulation of almost all Rab6/NPY vesicles present in the cell (Supplementary Figure S6B). These data suggest that increasing amounts of BICDR-1 in cells shift the transport of Rab6/NPY secretory vesicles to the microtubule minus-end (retrograde) direction.

In young neurons, BICDR-1 coincides with NPY-GFP-positive vesicles in the cell body and neurites (Figure 5E) and endogenous Rab6 (Rab6A and Rab6B) co-localize with NPY-GFP in a similar manner (Figure 5F). Consistent with the Hela cell data, expression of GFP-BICDR-1 in DIV3 neurons causes a strong accumulation of dynein/dynactin (Supplementary Figure S7A and B) and Rab6A and Rab6B-positive vesicles in the soma (Figure 6A; Supplementary Figure S7C and D), whereas other trafficking markers, such as endosomes were unaffected (Supplementary Figure S7E). Quantification showed an ~3-fold increase in Rab6A and Rab6B fluorescent staining intensity in the cell bodies of BICDR-1-transfected neurons compared with surrounding non-transfected control neurons (Figure 6B). Moreover, expression of BICDR-1 strongly accumulates NPY-GFP-positive secretory vesicles in the soma and caused a marked decrease in the number of NPY-GFP vesicles in developing neurites, compared with

control cells (Figure 6C and D). Similar results were obtained with other neuronal secretory vesicle markers, such as GFP-Sema3A and BDNF-GFP (Figure 6D; Supplementary Figure S7F and G). Together these data suggest that BICDR-1 controls the trafficking of secretory vesicles most likely by shifting the transport balance towards the retrograde direction. As a result, Rab6/BICDR-1 secretory vesicles concentrate in the cell body and trafficking into growing neurites is blocked.

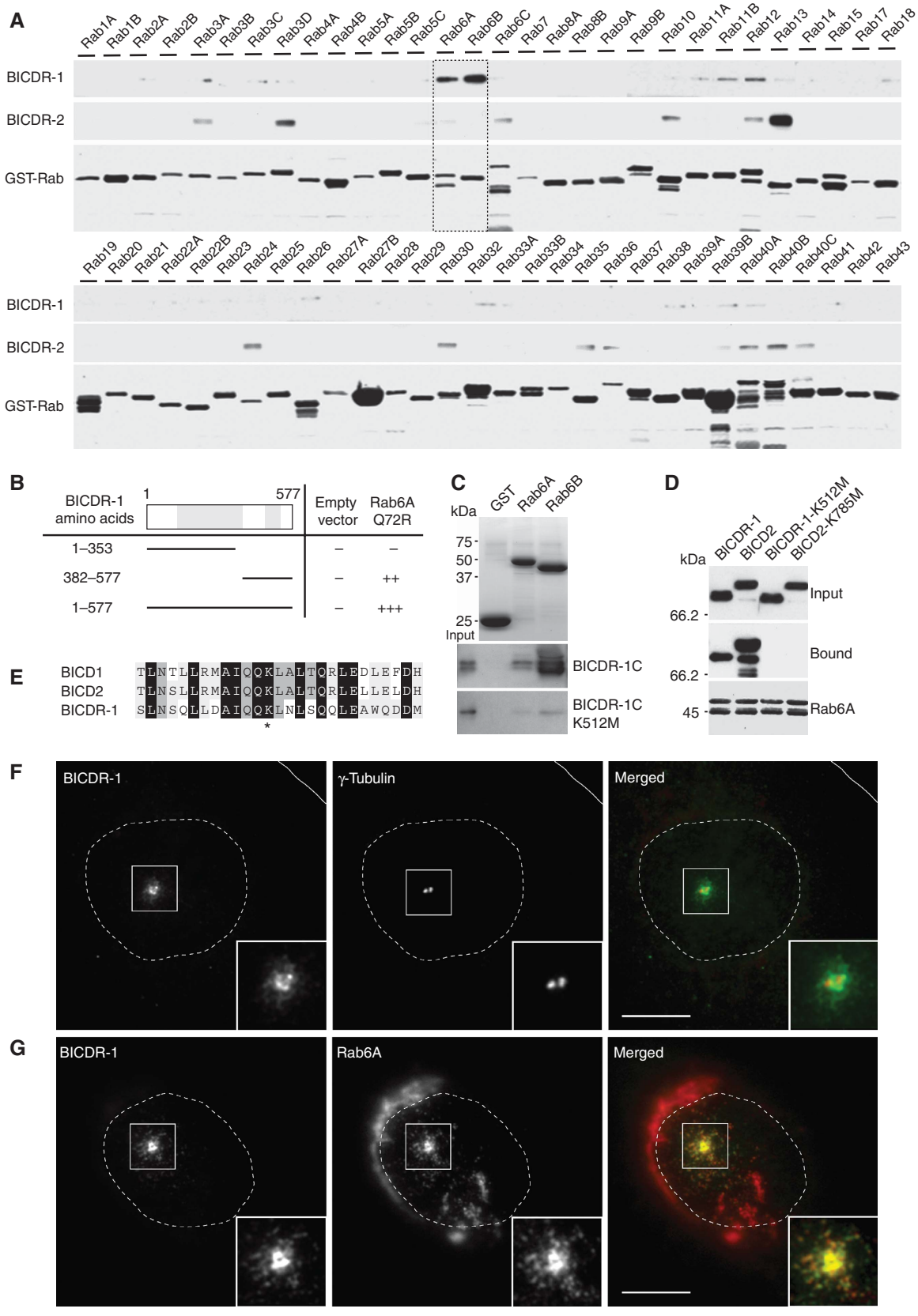

BICDR-1 does not alter secretory vesicle exocytosis in neurons

We next examined whether BICDR-1 also regulates secretory vesicle exocytosis, which, in neurons, occurs after neuronal depolarization with 60 mM KCl (de Wit *et al*, 2009). Live imaging showed that in both control and BICDR-1-expressing neurons transient NPY-GFP exocytotic events occur after KCl-induced depolarization (Figure 6E and F). Quantification showed that the NPY-GFP secretion events in control and BICDR-1-expressing neurons have similar kinetics (Figure 6F). However, secretory vesicle fusion is seen at a different subcellular location in BICDR-1-expressing neurons. Most NPY-GFP exocytotic events occur in the cell body of BICDR-1 neurons, whereas in control cells most events take place in developing neurites. These data are consistent with the observed accumulates of secretory vesicles in the soma and decreased numbers in neurites in BICDR-1 neurons. In fibroblast cells, quantitative analysis of location of the exocytotic events (red dots; Supplementary Figure S6D) showed that in BICDR-1 cells most secretion took place around the pericentrosomal region, whereas in control cells most events occurred at the periphery (Supplementary Figure S6C–F; Supplementary Movies S3 and S4). Together these data suggest that BICDR-1 does not influence secretory vesicle exocytosis but controls the distribution of secretory carriers.

Kif1C participates in transport of secretory vesicles in neurons

Most secretory vesicles in neurons exhibit bi-directional motility movements (de Wit *et al*, 2006). The observed retrograde movement of secretory vesicles in young neurons is likely caused by the interaction between BICDR-1/Rab6 and the dynein–dynactin complex (Figure 4; Supplementary Figure S7), whereas the anterograde movement is most likely explained by the binding of microtubule plus-end-directed kinesin motors. We have shown earlier that kinesin motor kinesin-1/Kif5 associates with BICD and participates in anterograde Rab6 secretory vesicles transport (Grigoriev *et al*, 2007). Here, we performed a yeast two-hybrid screen for BICDR-1 partners and found Kif1C as a potential interacting protein (Figure 7A). Both full-length BICDR-1 and an N-terminal region of BICDR-1, amino acids 1–353, interact with the C-terminal tail domain of Kif1C, amino acids 811–1090 and not with other tail regions of Kif1C or other kinesin motors, such as Kif5 (Figure 7A; data not shown). This interaction was further supported by co-immunoprecipitation of endogenous Kif1C by overexpressed BICDR-1 in Hela cells (Figure 7B). Moreover, expression of GFP-BICDR-1 in Vero cells and primary neurons caused strong accumulation of endogenous Kif1C at the pericentrosomal region (Figure 7C and D). BICDR-1 expression has no effect on endogenous Kif5 staining (data not shown). These results show that BICDR-1 regulates recruitment and/or activity of the anterograde kinesin motor Kif1C on Rab6 secretory carriers.

Next, we tested whether the secretory vesicle distribution in neurons depends on Kif1C function. Neurons transfected with Kif1C-shRNA accumulate NPY-GFP-positive secretory vesicles in the cell body and showed a strong decrease in the number of NPY-GFP vesicles in developing neurites (Figure 7E and F), consistent with a role for Kif1C in the anterograde movement of Rab6 secretory vesicles. Together these data indicate that the association of BICDR-1 with Rab6, Kif1C and dynein/dynactin is likely to contribute to the bi-directional motility of secretory vesicles in young neurons.

BICDR-1 regulates neurite outgrowth

As BICDR-1 expression in developing neurons strongly decreases after a few days in culture, we investigated the effect of sustained BICDR-1 expression on neuronal development. Neurons were transfected with GFP-BICDR-1 at DIV0.25 together with β-galactosidase as a marker to visualize neuronal morphology. At 2, 3 and 4 days after transfection, BICDR-1-transfected neurons showed a marked reduction in neurite outgrowth compared with control cells transfected with an empty vector and β-galactosidase (Figure 8A and B). The total neurite length was decreased by $>50\%$ in BICDR-1-expressing neurons at DIV3 (Figure 8C). No significant difference was observed in BICD1- or BICD2-expressing neurons (Figure 8A and G). Co-staining for the dendritic marker MAP2 and axonal protein Tau-1 showed that both developing dendrites and axon were significantly shortened (Figure 8E and F), suggesting that sustained BICDR-1 expression inhibits total neurite development.

We hypothesized that the observed neurite phenotype was due to BICDR-1-mediated Rab6 secretory vesicle accumulation in the cell body. Neurons transfected with Rab6A-shRNA, Rab6B-shRNA or both (Supplementary Figure S8) show a $\sim 50\%$ reduction of total neurite length compared with control cells (Figure 8B and I), suggesting that both Rab6A and Rab6B have an important function in neurite outgrowth. To interfere with the interaction between BICDR-1 and Rab6, we overexpressed the Rab6-binding domain of BICDR-1 (BICDR-1C), which forms small clusters that strongly recruit Rab6A and Rab6B (data not shown) and observed a marked decrease in neurite outgrowth (Figure 8D). Importantly, the BICDR-1C-K512M mutant does not affect Rab6A/B

Figure 3 BICDR-1 binds Rab6A/B and is localized pericentrosomally. (**A**) GST pull-down assay with GST-Rabs (Rab1–43) and extracts of Cos7 cells expressing Flag-BICDR-1 or Flag-BICDR-2. Flag-tagged proteins were detected by western blotting with antibodies against Flag; GST proteins were visualized using Amido Black. (**B**) Yeast two-hybrid analysis. Rab6A-Q72R was linked to LexA and BICDR-1 (1–577), (1–353) or (382–577) was fused to a GAL4 activation domain. Interaction strength was scored according to the time needed for a β-galactosidase reporter to generate visible blue-coloured yeast colonies on X-Gal containing filters in a colony filter lift assay: $+++$ 0–30 min, $++$ 30–60 min, $+$ 60–180 min and $-$ no β-galactosidase activity. (**C**) *In vitro* binding assay using purified GST-Rab6A/B bound to beads and purified His-BICDR-1C or His-BICDR-1C-K512M. His-tagged proteins were detected by western blotting with antibodies against His; GST-Rab6A/B was visualized by Coomassie staining. (**D**) GST pull-down assay with GST-Rab6A and extracts of Cos7 cells expressing Flag-BICDR-1, Flag-BICD2, Flag-BICDR-1-K512M or Flag-BICD2-K785M. Flag-tagged proteins were detected by western blotting with antibodies against Flag; GST-Rab6A was visualized using Amido Black. (**E**) Sequence alignment of BICD1, BICD2 and BICDR-1 Rab6-binding region (* indicates site of BICD2-K785M and BICDR-1-K512M mutations). (**F**) Co-staining of BICDR-1 (green) and γ-tubulin (red) in a Vero cell. (**G**) Representative image of a Vero cell co-stained for endogenous BICDR-1 (green) and Rab6A (red). (**F–G**) Solid lines indicate the cell edge and dashed lines indicate the nucleus. The insets show magnifications of boxed areas. Scale bars, 10 μm.

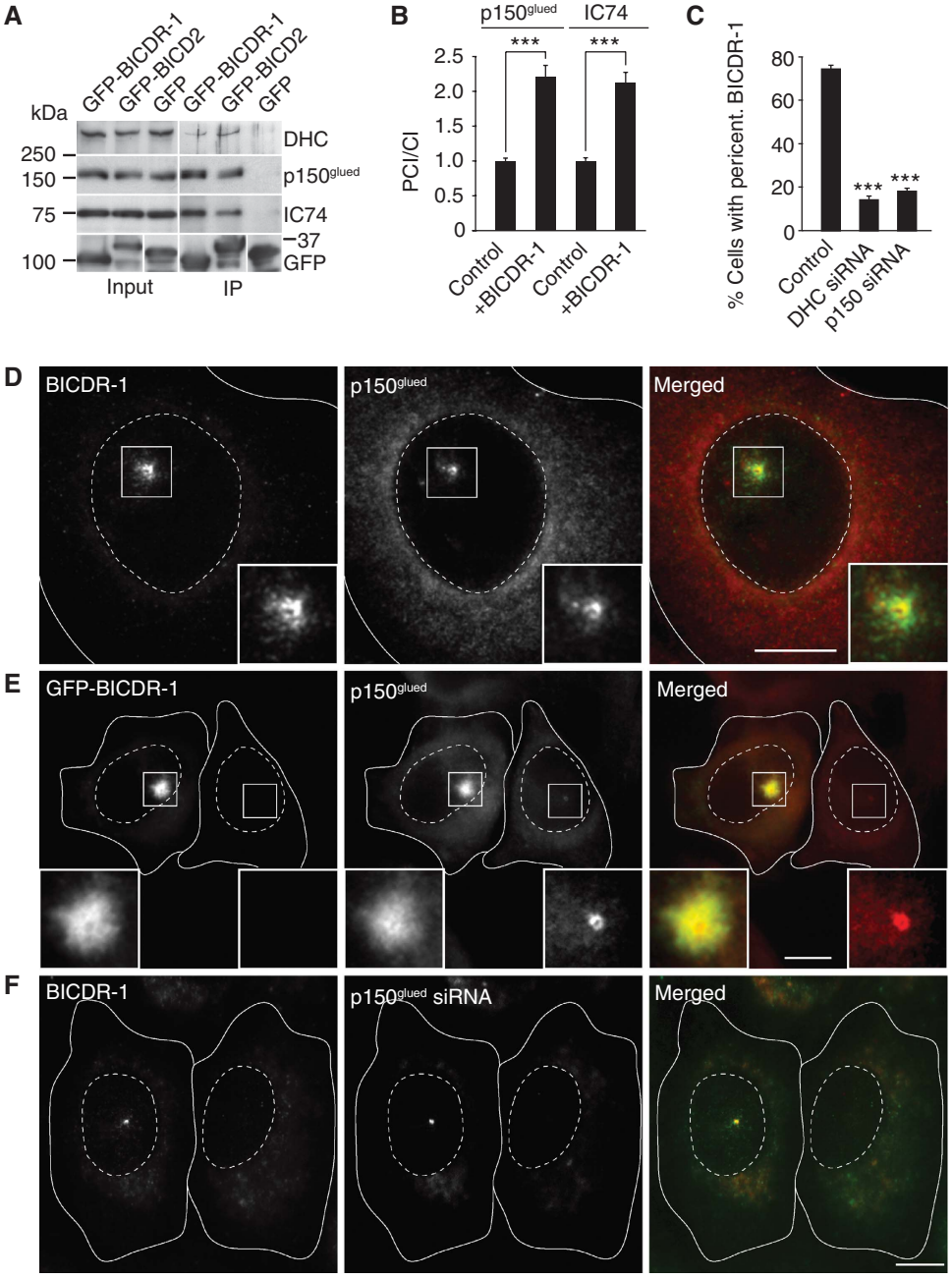

Figure 4 BICDR-1 interacts with the dynein/dynactin motor complex. (**A**) Immunoprecipitations from extracts of Hela cells transfected with the indicated constructs and probed for DHC, p150^{glued} or dynein intermediate chain 74 (IC74). (**B**) Ratio of pericentrosomal versus cytoplasmic p150^{glued} or IC74 fluorescence intensity in cells with and without GFP-BICDR-1 overexpression (average ± s.e.m.; p150^{glued} control, $n=29$; p150^{glued} + BICDR-1, $n=30$; IC74 control, $n=32$; IC74 + BICDR-1, $n=19$ cells). (**C**) Percentage of cells, transfected with indicated siRNAs, with endogenous pericentrosomal BICDR-1 (average ± s.e.m.; control, $n=3040$; DHC siRNA, $n=533$; p150^{glued}, $n=792$ cells). (**D**) Representative image of a Vero cell stained for endogenous BICDR-1 (green) and for p150^{glued} (red). (**E**) Representative image of Hela cells with and without GFP-BICDR-1 (green) overexpression stained for p150^{glued} (red). (**F**) Vero cells transfected with p150^{glued}-specific siRNA (right) and untransfected (left). Stained for BICDR-1 (green) and p150^{glued} (red). (**D–F**) Solid lines indicate the cell edge and dashed lines indicate the nucleus. The insets show magnifications of boxed areas. Scale bars, 10 μm. ***$P<0.001$.

distribution (data not shown) and neurite length (Figure 8D). Furthermore, disruption of the dynein/dynactin motor complex by overexpression of GFP-p50 or GFP-p150CC1 and knockdown of Kif1C also resulted in a reduction in neurite outgrowth (Figure 8A, H and I). Taken together these data suggest that altered Rab6-, Kif1C- and dynein-dependent secretory vesicle trafficking likely cause the morphological abnormality observed in developing neurons with sustained BICDR-1 expression.

Discussion

Here, we describe a molecular mechanism in which a new BICD family protein, named BICDR-1, regulates secretory

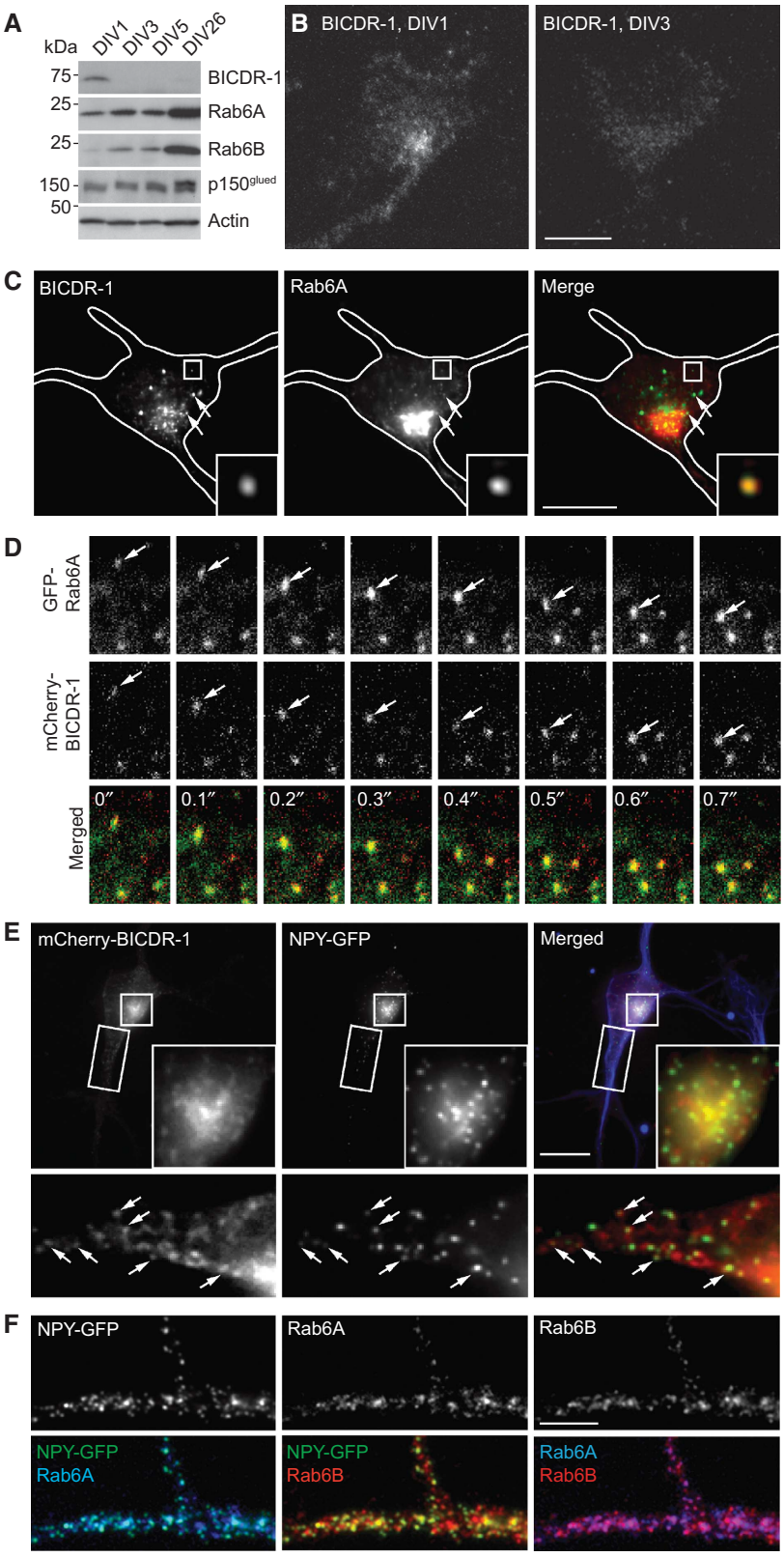

Figure 5 BICDR-1 is expressed during early stages of neuronal development and is associated with Rab6-positive secretory vesicles in neurons. (**A**) Developmental expression of BICDR-1, Rab6A, Rab6B, p150^{glued} and actin in cultured hippocampal neurons at DIV1, DIV3, DIV5 and DIV26. (**B**) Immunofluorescent images of BICDR-1 in hippocampal neurons at DIV1 (left) and DIV3 (right). (**C**) DIV1 neuron fixed and stained for BICDR-1 (green) and Rab6A (red). (**D**) Time-lapse images of a DIV2 neuron transfected with mCherry-BICDR-1 (red) and GFP-Rab6A. Time indicated in seconds. (**E**) DIV2 + 2 hippocampal neuron transfected with mCherry-BICDR-1 (red) and NPY-GFP (green) and stained for Tuj1 (blue). The insets show magnifications of the boxed areas, arrows indicate co-localization (Pearson's coefficient, $r_p = 0.8$). (**F**) Detail of DIV1 + 3 hippocampal neuron transfected with NPY-GFP (green) and stained for Rab6A (blue) and Rab6B (red). Merged images show co-localization of NPY-GFP/Rab6A ($r_p = 0.9$), NPY-GFP/Rab6B ($r_p = 0.8$) and Rab6A/Rab6B ($r_p = 0.8$). (**B**, **C**, **E**) Solid lines indicate the cell edge; the insets show magnifications of boxed areas and arrows indicate co-localization. Scale bars, 10 μm. (**F**) Scale bar, 5 μm.

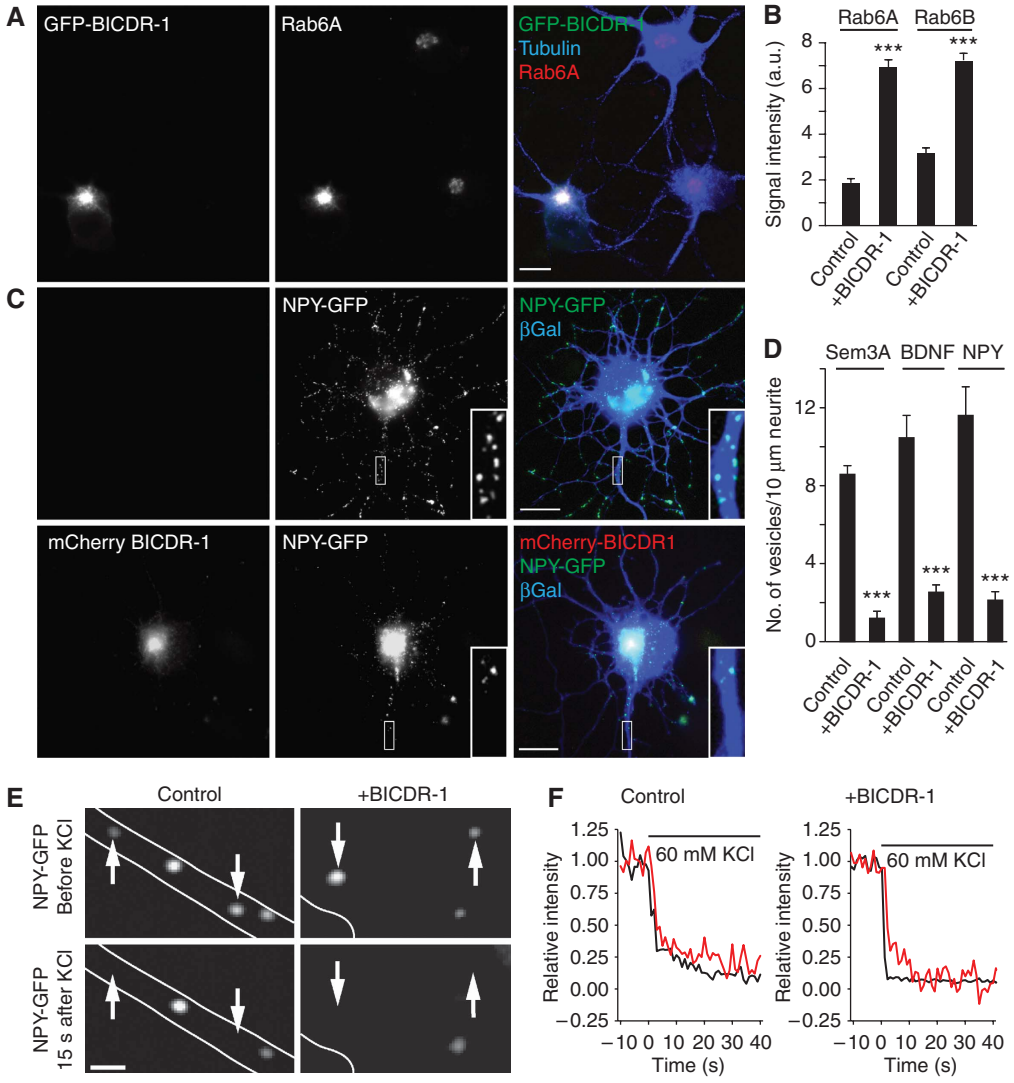

Figure 6 BICDR-1 controls the trafficking of secretory vesicles in neurons. (**A**) Representative image of hippocampal neurons transfected with GFP-BICDR-1 (green) and stained for Rab6A (red) and α-tubulin (blue). (**B**) Quantification of Rab6A and Rab6B immunostaining intensities in hippocampal neurons transfected with GFP-BICDR-1 (average ± s.e.m.; Rab6A control, $n=21$; Rab6A + BICDR-1, $n=10$; Rab6B control, $n=31$; Rab6B + BICDR-1, $n=16$ cells). (**C**) DIV2 + 2 hippocampal neurons transfected with either NPY-GFP (green) and β-Gal (blue; top row) or NPY-GFP (green), mCherry-BICDR-1 (red) and β-Gal (blue; bottom row). (**D**) Quantification of the number of GFP-labelled vesicles per 10 μm neurite in DIV2 + 2 hippocampal neurons transfected with indicated constructs (average ± s.e.m.; Sem3A control, $n=10$; Sem3A + BICDR-1, $n=10$; BDNF control, $n=5$; BDNF + BICDR-1, $n=5$; NPY control, $n=5$; NPY + BICDR-1, $n=5$). (**E**) Time-lapse images of DIV4 + 1 hippocampal neurons transfected with NPY-GFP and mCherry (control, axon) or NPY-GFP, mCherry and HA-BICDR-1 (+BICDR-1, cell body) before and after stimulation by addition of KCl (60 mM final concentration). Scale bar, 1 μm; arrows indicate secreting vesicles; solid lines indicate the cell edge. (**F**) Fluorescence intensity traces of secretory events in the axon (control) or cell body (+BICDR-1) during KCl addition. ***$P<0.001$.

trafficking in developing neurons. BICDR-1 interacts with Rab6, Kif1C and the dynein/dynactin motor complex, and coordinates trafficking of Rab6/NPY-positive secretory vesicles. BICDR-1 expression is regulated during embryonic development and controls neuronal differentiation. At early developmental stages, pericentrosomal BICDR-1 restricts secretory transport and inhibits neuritogenesis, whereas later during neuronal development the reduction in BICDR-1 expression permits anterograde transport required for neurite outgrowth.

BICDR-1 controls secretory trafficking in young neurons

Each organelle carries its own set of small Rab GTPases, which ensures the specificity of intracellular membrane transport. Several studies indicate that Rab GTPases and their effectors are key regulators in vesicular trafficking (Zerial and McBride, 2001; Schlager and Hoogenraad, 2009; Stenmark, 2009). Here, we show that BICDR-1 is a Rab6 effector, recruits dynein/dynactin and Kif1C to Rab6/NPY-positive secretory vesicles and controls the trafficking and distribution of these carriers. We suggest a model in which BICDR-1 functions as a linker between cargo and motor proteins, with the C-terminus bound to the Rab6 secretory vesicles and the N-terminus bound to the dynein/dynactin complex and Kif1C motor and controls secretory vesicle transport. Although BICD family proteins are known to be conserved motor adaptor proteins for Rab6 cargos (Hoogenraad *et al*, 2001; Matanis *et al*, 2002; Coutelis and

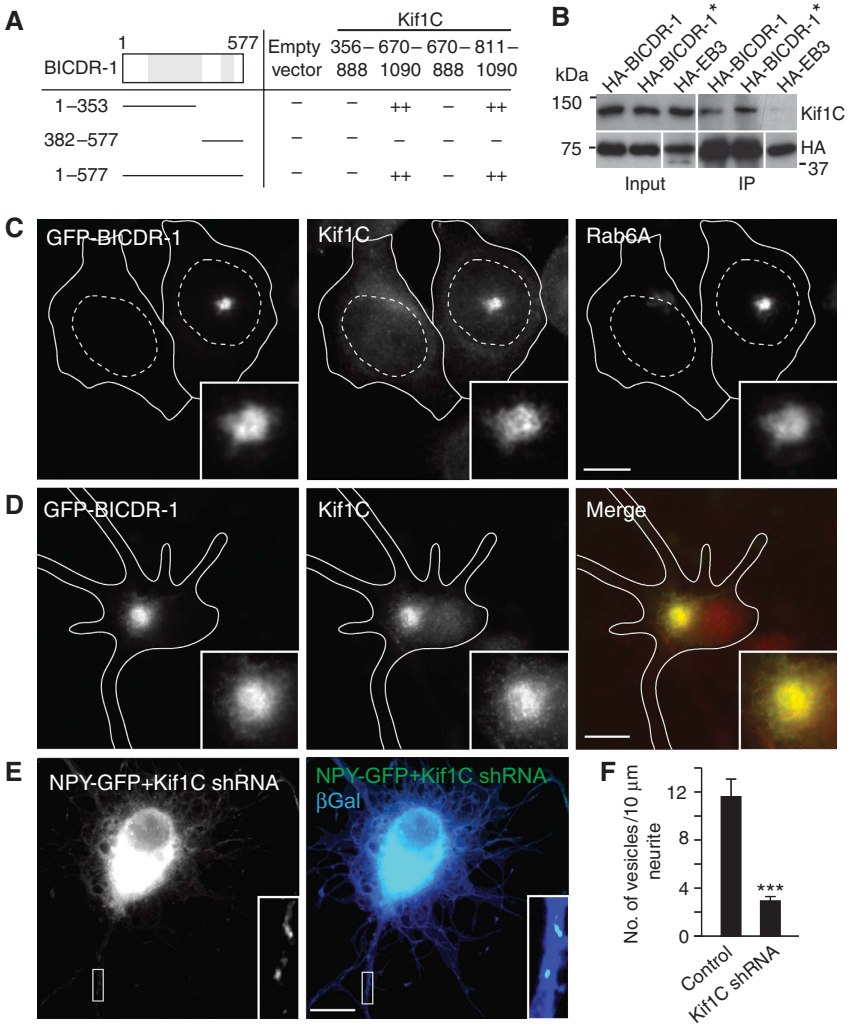

Figure 7 BICDR-1 interacts with Kif1C. (**A**) Yeast two-hybrid analysis. Kif1C (356–888), (670–1090), (670–888) or (811–1090) was linked to LexA and BICDR-1 (1–577), (1–353) or (382–577) was fused to a GAL4 activation domain. Interaction strength was scored according to the time needed for β-galactosidase reporter to generate visible blue-coloured yeast colonies on X-Gal containing filters in a colony filter lift assay: + + + 0–30 min, + + 30–60 min, + 60–180 min and − no β-galactosidase activity. (**B**) Immunoprecipitations from extracts of Hela cells transfected with the indicated constructs and probed for Kif1C (* indicates that cells were treated with 1 μM staurosporin for 1 h before immunoprecipitation). (**C**) Representative image of Hela cells with and without GFP-BICDR-1 overexpression stained for Kif1C and Rab6A. (**D**) DIV2 + two hippocampal neuron transfected with GFP-BICDR-1 (green) and stained for Kif1C (red). (**E**) DIV1 + three hippocampal neurons transfected with either NPY-GFP (green), Kif1C shRNA and β-Gal (blue). (**F**) Quantification of the number of GFP-labelled vesicles per 10 μm neurite in DIV1 + three hippocampal neurons transfected with indicated constructs (average ± s.e.m.; control, $n = 5$; NPY + Kif1C shRNA, $n = 6$). (**C**–**E**) Solid lines indicate the cell edge and dashed lines indicate the nucleus. The insets show magnifications of boxed areas. Scale bars, 10 μm. ***$P < 0.001$.

Ephrussi, 2007; Januschke *et al*, 2007), the effects of BICDR-1 on the distribution of Rab6 vesicles are remarkably distinct from other BICD family proteins; while BICD/Rab6-positive carriers are transported to the cell periphery (Grigoriev *et al*, 2007), BICDR-1-bound Rab6 vesicles accumulate at pericentrosomal region. We found a strong correlation between the level of BICDR-1 expression and the amount of Rab6 secretory vesicles around the centrosome. At low-level BICDR-1 expression most Rab6 secretory vesicles are observed throughout the cytoplasm with only a few vesicles concentrated around the centrosome (Supplementary Figure S6A), whereas adding increasing amounts of BICDR-1 leads to robust accumulation of Rab6 secretory vesicles in the pericentrosomal region (Supplementary Figure S6B). These data suggest that BICDR-1 may control the trafficking of secretory vesicles by changing the transport balance towards the microtubule minus-end (retrograde) direction. Moreover, BICDR-1 competes with BICD for Rab6 in *in vitro* assays and may control bi-directional Rab6 secretory transport in developing neurons. We hypothesize that by changing the molecular ratios of BICD/BICDR-1 on Rab6 vesicles during neuronal differentiation, the direction and distribution of secretory vesicle transport could be altered.

It is well known that direction of transport strongly depends on the net balance between microtubule plus-end- and minus-end-directed motors (Welte, 2004; Wang and Schwarz, 2009). We have shown earlier that dynein/dynactin and kinesin-1/Kif5 bind to BICD and participate in bi-directional Rab6 vesicle trafficking (Hoogenraad *et al*, 2001; Grigoriev *et al*, 2007). However, this is probably not the complete picture, several other interactions between Rab6, BICD, dynein/dynactin and kinesins have been reported. Rab6

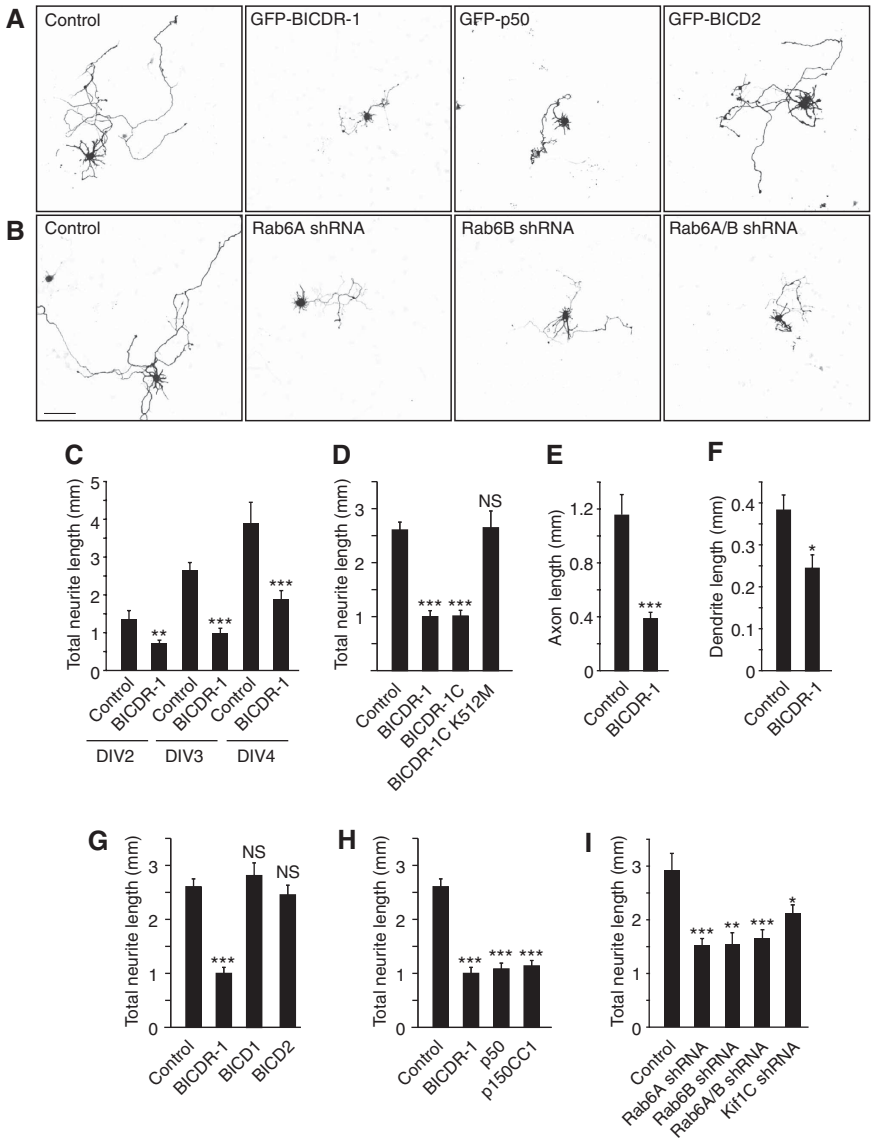

Figure 8 BICDR-1 regulates neurite outgrowth. (**A**, **B**) Hippocampal neurons co-transfected at DIV0.25 with indicated constructs and β-Gal to visualize morphology, fixed at DIV3. Scale bar, 100 μm. (**C**) Total neurite length after 2-, 3- or 4-day overexpression of GFP-BICDR-1 or an empty pGW1-HA vector as control (DIV2 control $n=9$, BICDR-1 $n=14$; DIV3 control $n=11$, BICDR-1 $n=12$; DIV4 control $n=14$, BICDR-1 $n=16$). (**D**) Total neurite length after 3-day overexpression of GFP-BICDR-1, GFP-BICDR-1C or GFP-BICDR-1C-K512M. Control cells were transfected with an empty pGW1-HA vector (control $n=37$; BICDR-1 $n=23$; BICDR-1C $n=15$; BICDR-1C-K512M $n=11$). (**E**) Axon length after 3-day overexpression of GFP-BICDR-1 or an empty pGW1-HA vector as control (control $n=9$; BICDR-1 $n=9$). (**F**) Dendrite length after 3-day overexpression of GFP-BICDR-1 or an empty pGW1-HA vector as control (control $n=14$; BICDR-1 $n=9$). (**G**) Total neurite length after 3-day overexpression of GFP-BICDR-1 or GFP-BICD2. Control cells were transfected with an empty pGW1-HA vector (control $n=37$; BICDR-1 $n=23$; BICD1 $n=12$; BICD2 $n=19$). (**H**) Total neurite length after 3-day overexpression of GFP-BICDR-1, GFP-p50 or GFP-p150CC1. Control cells were transfected with an empty pGW1-HA vector (control $n=37$; BICDR-1 $n=23$; p50 $n=15$; p150CC1 $n=17$). (**I**) Total neurite length after 3-day overexpression of shRNA specific for Rab6A, Rab6B, Rab6A and Rab6B or Kif1C. Control cells were transfected with an empty pSuper vector (control $n=14$; Rab6A shRNA $n=21$; Rab6B shRNA $n=10$; Rab6A/B shRNA $n=16$; Kif1C shRNA $n=13$). (**C**–**I**) Average ± s.e.m., $^{*}P<0.05$. $^{**}P<0.01$. $^{***}P<0.001$.

directly interacts with kinesin motor protein Rab6kinesin/mklp2 and dynein/dynactin (Echard *et al*, 1998; Short *et al*, 2002; Wanschers *et al*, 2008), dynactin also controls kinesin motor transport (Deacon *et al*, 2003; Colin *et al*, 2008) and BICD proteins are involved in several transport processes independent of Rab6 (Houalla *et al*, 2005; Larsen *et al*, 2008; Dienstbier *et al*, 2009). Here, we show that BICDR-1 does not interact with Kif5 but recruits kinesin-3/Kif1C to Rab6 secretory vesicles in hippocampal neurons. These data suggest that the association of BICDR-1 with Rab6, Kif1C and dynein/dynactin is likely to contribute to the bi-directional motility of secretory vesicles in young neurons. However it is expected that additional motor proteins, coordinating factors and signalling proteins will participate in regulating anterograde secretory vesicle trafficking in neurons. Interesting in this respect are the recent data on the adaptor protein RILP that requires Rab7, dynein/dynactin and several regulatory proteins to fully assemble in a functional motor–cargo–adaptor complex (Johansson *et al*, 2007) and the observation that phosphorylated huntingtin promotes anterograde transport of BDNF-positive vesicles by recruiting kinesin-1 to the dynactin complex (Colin *et al*, 2008).

It is tempting to speculate that BICDR-1 is a coordinator of bi-directional transport and responsible for setting the balance in the microtubule minus-end direction. Interestingly, BICDR-1 overexpression accumulates Kif1C in the cell body suggesting that minus-end-directed motor dynein has a dominant role in mediating BICDR-1/Rab6 vesicle transport. It is possible that Kif1C is a weak motor in the context of BICDR-1 and has a more active role in Rab6 vesicles transport at later stages of neuronal development independent of BICDR-1. Consistently, mutant screens in *Drosophila* and *Caenorhabditis elegans* show that Unc-104/kinesin-3 is the major contributor to anterograde transport of neuropeptide-filled vesicles in differentiated neurons (Zahn *et al*, 2004; Barkus *et al*, 2008). In several model systems other factors, such as Klar and Halo, have been identified that change bi-directional mobility (Welte, 2004). It is also possible that BICDR-1 is not solely involved in motor coordination but also binds to pericentrosomal components and thereby assists in stabilizing and concentrating secretory vesicles around the centrosome. Consistently, BICDR-1 pull-down assays combined with mass spectrometry analysis showed strong enrichment of several centrosomal proteins (data not shown). Additional studies are required to determine the precise role for BICDR-1 in bi-directional secretory vesicle trafficking and centrosomal anchoring. Regardless of the underlying mechanism, in this study we show that BICDR-1 controls the subcellular distribution of Rab6 secretory vesicles. Changing the trafficking of secretory vesicles and thereby the location of secretory exocytotic events may have important morphogenetic consequences; for example, by determining where new membrane and membrane-associated proteins will be added during highly controlled developmental processes, such as neuronal differentiation.

Regulation of neuronal development by BICDR-1

The secretory pathway is a conserved mechanism that targets proteins destined for secretion or integration into the plasma membrane in a highly regulated manner (Bonifacino and Glick, 2004). Studies in various model organisms have provided strong evidence that secretory trafficking is important for neuronal development (Hanus and Ehlers, 2008; Pfenninger, 2009). We propose that BICDR-1 is a regulator of Rab6 secretory vesicle transport and controls the timing of neurite outgrowth (Supplementary Figure S9). Several lines of evidence support this model. First, BICDR-1 is predominantly present in undifferentiated neural tissue in young embryos and its expression rapidly declines during neuronal development. Second, BICDR-1 redistributes Rab6/NPY secretory vesicles out of the neurites into the cell body and controls the localization of NPY-GFP secretion events. Similar results were obtained with other neuronal secretory vesicle proteins, such as GFP-Sema3A and BDNF-GFP. Neurons with sustained BICDR-1 expression show a decrease in neurite outgrowth and knockdown of Rab6A and Rab6B mimic the effect. Thus, BICDR-1 acts in a secretory transport pathway in developing neurons and thereby regulates neurite outgrowth. This is consistent with previous observations in young neurons showing that membrane structures cluster together around the centrosome and vesicular transport precedes neurite formation (Higginbotham and Gleeson, 2007). We hypothesize that undifferentiated neurons collect BICDR-1/Rab6 secretory cargo around the centrosome and restricts secretory vesicle exocytosis to the cell body. On neuronal differentiation, fast neurite extensions require long-range secretory trafficking and localized secretion near growth cones (Pfenninger, 2009). At this stage, BICDR-1 expression is reduced and permits anterograde transport of Rab6 secretory vesicles and subsequent exocytosis in developing neurites. It is tempting to speculate that the BICDR-1 knockdown phenotype in zebrafish is caused by mistargeting of secretory cargo (Babb *et al*, 2005). Interestingly, an analogous model exists in cytotoxic T lymphocytes where delivery of secretory granules to the immunological synapse is controlled by the centrosome (Stinchcombe and Griffiths, 2007). This indicates that various molecular mechanisms exist, which control secretory cargo trafficking to ensure temporal and spatial regulation of secretion events.

In conclusion, we have identified BICDR-1 as a novel regulator of secretory vesicle trafficking in developing neurons. This work provides important mechanistic insights into the modulation of neuronal transport and highlights BICDR-1 as a regulatory factor that coordinates the direction of secretory cargo transport in differentiating neurons.

Materials and methods

Antibodies and DNA constructs

Mouse BICDR-1 is annotated under the accession number: GU973876. Rabbit anti-BICDR-1 antibodies were raised against GST-tagged BICDR-1 amino acids 1–146 (#12) and 161–387 (#13), other previously described antibodies used mouse anti-Rab6A/Rab6A' (Matanis *et al*, 2002) and BICD2 (Hoogenraad *et al*, 2001). The BICDR-1 constructs were generated by subcloning mouse BICDR-1 cDNA into pGW1- and pβactin-expression vectors. BICDR-1-shRNA complementary oligonucleotides were annealed and inserted into pSuper vector. See for details Supplementary Materials and methods.

Primary hippocampal neuron cultures and immunocytochemistry

Primary hippocampal cultures were prepared from embryonic day 18 (E18) rat brains as described earlier (Jaworski *et al*, 2009) and transfected using Lipofectamine 2000 (Invitrogen). Immunocytochemistry was performed as described in the Supplementary Materials and methods.

Image acquisition, processing and morphometric analyses

Confocal images of neurons were acquired using a Zeiss LSM 510 confocal laser-scanning microscope. Morphometric analysis and time-lapse live cell imaging was performed as described (Jaworski *et al*, 2009). See for details Supplementary Materials and methods.

In situ hybridization

Whole-mount *in situ* hybridization and *in situ* hybridization of cryosections were performed as described in Supplementary Materials and methods.

Zebrafish maintenance and microinjections

Fish were raised and kept under standard laboratory conditions at 28.5°C. BICDR-1 and mismatch MOs were injected into one-cell embryo to two-cell embryos. Subsequently embryos were staged and fixed as described in Supplementary Materials and methods.

Supplementary data

Supplementary data are available at *The EMBO Journal* Online (http://www.embojournal.org).

Acknowledgements

This work is supported by The Prinses Beatrix Fonds. EdG is supported by the Netherlands Organization for Health Research and Development (ZonMw-VIDI). AA is supported by the

Netherlands Organization for Scientific Research (NWO-ALW VICI) and the Netherlands Organization for Health Research and Development (ZonMw-TOP). CCH is supported by the Netherlands Organization for Scientific Research (NWO-ALW, NWO-ECHO), the Netherlands Organization for Health Research and Development (ZonMw-VIDI, ZonMw-TOP), European Science Foundation (European Young Investigators (EURYI) Award), EMBO Young Investigators Program (YIP) and Human Frontier Science Program Career Development Award (HFSP-CDA).

Conflict of interest

The authors declare that they have no conflict of interest.

References

Babb SG, Kotradi SM, Shah B, Chiappini-Williamson C, Bell LN, Schmeiser G, Chen E, Liu Q, Marrs JA (2005) Zebrafish R-cadherin (Cdh4) controls visual system development and differentiation. *Dev Dyn* **233:** 930–945

Barkus RV, Klyachko O, Horiuchi D, Dickson BJ, Saxton WM (2008) Identification of an axonal kinesin-3 motor for fast anterograde vesicle transport that facilitates retrograde transport of neuropeptides. *Mol Biol Cell* **19:** 274–283

Bonifacino JS, Glick BS (2004) The mechanisms of vesicle budding and fusion. *Cell* **116:** 153–166

Bradke F, Dotti CG (2000) Differentiated neurons retain the capacity to generate axons from dendrites. *Curr Biol* **10:** 1467–1470

Bullock SL, Ish-Horowicz D (2001) Conserved signals and machinery for RNA transport in Drosophila oogenesis and embryogenesis. *Nature* **414:** 611–616

Caviston JP, Holzbaur EL (2006) Microtubule motors at the intersection of trafficking and transport. *Trends Cell Biol* **16:** 530–537

Claussen M, Suter B (2005) BicD-dependent localization processes: from Drosophilia development to human cell biology. *Ann Anat* **187:** 539–553

Colin E, Zala D, Liot G, Rangone H, Borrell-Pages M, Li XJ, Saudou F, Humbert S (2008) Huntingtin phosphorylation acts as a molecular switch for anterograde/retrograde transport in neurons. *EMBO J* **27:** 2124–2134

Conde C, Caceres A (2009) Microtubule assembly, organization and dynamics in axons and dendrites. *Nat Rev Neurosci* **10:** 319–332

Coutelis JB, Ephrussi A (2007) Rab6 mediates membrane organization and determinant localization during Drosophila oogenesis. *Development* **134:** 1419–1430

de Wit J, Toonen RF, Verhaagen J, Verhage M (2006) Vesicular trafficking of semaphorin 3A is activity-dependent and differs between axons and dendrites. *Traffic* **7:** 1060–1077

de Wit J, Toonen RF, Verhage M (2009) Matrix-dependent local retention of secretory vesicle cargo in cortical neurons. *J Neurosci* **29:** 23–37

Deacon SW, Serpinskaya AS, Vaughan PS, Lopez Fanarraga M, Vernos I, Vaughan KT, Gelfand VI (2003) Dynactin is required for bidirectional organelle transport. *J Cell Biol* **160:** 297–301

Dienstbier M, Boehl F, Li X, Bullock SL (2009) Egalitarian is a selective RNA-binding protein linking mRNA localization signals to the dynein motor. *Genes Dev* **23:** 1546–1558

Echard A, Jollivet F, Martinez O, Lacapere JJ, Rousselet A, Janoueix-Lerosey I, Goud B (1998) Interaction of a Golgi-associated kinesin-like protein with Rab6. *Science* **279:** 580–585

Echard A, Opdam FJ, de Leeuw HJ, Jollivet F, Savelkoul P, Hendriks W, Voorberg J, Goud B, Fransen JA (2000) Alternative splicing of the human Rab6A gene generates two close but functionally different isoforms. *Mol Biol Cell* **11:** 3819–3833

Erez H, Malkinson G, Prager-Khoutorsky M, De Zeeuw CI, Hoogenraad CC, Spira ME (2007) Formation of microtubule-based traps controls the sorting and concentration of vesicles to restricted sites of regenerating neurons after axotomy. *J Cell Biol* **176:** 497–507

Fukuda M (2008) Regulation of secretory vesicle traffic by Rab small GTPases. *Cell Mol Life Sci* **65:** 2801–2813

Grigoriev I, Splinter D, Keijzer N, Wulf PS, Demmers J, Ohtsuka T, Modesti M, Maly IV, Grosveld F, Hoogenraad CC, Akhmanova A (2007) Rab6 regulates transport and targeting of exocytotic carriers. *Dev Cell* **13:** 305–314

Hanus C, Ehlers MD (2008) Secretory outposts for the local processing of membrane cargo in neuronal dendrites. *Traffic* **9:** 1437–1445

Higginbotham HR, Gleeson JG (2007) The centrosome in neuronal development. *Trends Neurosci* **30:** 276–283

Hirokawa N, Noda Y (2008) Intracellular transport and kinesin superfamily proteins, KIFs: structure, function, and dynamics. *Physiol Rev* **88:** 1089–1118

Hirokawa N, Takemura R (2005) Molecular motors and mechanisms of directional transport in neurons. *Nat Rev Neurosci* **6:** 201–214

Hoogenraad CC, Akhmanova A, Howell SA, Dortland BR, De Zeeuw CI, Willemsen R, Visser P, Grosveld F, Galjart N (2001) Mammalian Golgi-associated Bicaudal-D2 functions in the dynein-dynactin pathway by interacting with these complexes. *EMBO J* **20:** 4041–4054

Hoogenraad CC, Wulf P, Schiefermeier N, Stepanova T, Galjart N, Small JV, Grosveld F, de Zeeuw CI, Akhmanova A (2003) Bicaudal D induces selective dynein-mediated microtubule minus end-directed transport. *EMBO J* **22:** 6004–6015

Houalla T, Hien Vuong D, Ruan W, Suter B, Rao Y (2005) The Ste20-like kinase misshapen functions together with Bicaudal-D and dynein in driving nuclear migration in the developing drosophila eye. *Mech Dev* **122:** 97–108

Januschke J, Nicolas E, Compagnon J, Formstecher E, Goud B, Guichet A (2007) Rab6 and the secretory pathway affect oocyte polarity in Drosophila. *Development* **134:** 3419–3425

Jaworski J, Kapitein LC, Gouveia SM, Dortland BR, Wulf PS, Grigoriev I, Camera P, Spangler SA, Di Stefano P, Demmers J, Krugers H, Defilippi P, Akhmanova A, Hoogenraad CC (2009) Dynamic microtubules regulate dendritic spine morphology and synaptic plasticity. *Neuron* **61:** 85–100

Johansson M, Rocha N, Zwart W, Jordens I, Janssen L, Kuijl C, Olkkonen VM, Neefjes J (2007) Activation of endosomal dynein motors by stepwise assembly of Rab7-RILP-p150Glued, ORP1L, and the receptor betalll spectrin. *J Cell Biol* **176:** 459–471

Kardon JR, Vale RD (2009) Regulators of the cytoplasmic dynein motor. *Nat Rev Mol Cell Biol* **10:** 854–865

Larsen KS, Xu J, Cermelli S, Shu Z, Gross SP (2008) BicaudalD actively regulates microtubule motor activity in lipid droplet transport. *PLoS One* **3:** e3763

Macaskill AF, Rinholm JE, Twelvetrees AE, Arancibia-Carcamo IL, Muir J, Fransson A, Aspenstrom P, Attwell D, Kittler JT (2009) Miro1 is a calcium sensor for glutamate receptor-dependent localization of mitochondria at synapses. *Neuron* **61:** 541–555

Matanis T, Akhmanova A, Wulf P, Del Nery E, Weide T, Stepanova T, Galjart N, Grosveld F, Goud B, De Zeeuw CI, Barnekow A, Hoogenraad CC (2002) Bicaudal-D regulates COPI-independent Golgi-ER transport by recruiting the dynein-dynactin motor complex. *Nat Cell Biol* **4:** 986–992

Navarro C, Puthalakath H, Adams JM, Strasser A, Lehmann R (2004) Egalitarian binds dynein light chain to establish oocyte polarity and maintain oocyte fate. *Nat Cell Biol* **6:** 427–435

Pfenninger KH (2009) Plasma membrane expansion: a neuron's Herculean task. *Nat Rev Neurosci* **10:** 251–261

Ran B, Bopp R, Suter B (1994) Null alleles reveal novel requirements for Bic-D during Drosophila oogenesis and zygotic development. *Development* **120:** 1233–1242

Schlager MA, Hoogenraad CC (2009) Basic mechanisms for recognition and transport of synaptic cargos. *Mol Brain* **2:** 25

Short B, Preisinger C, Schaletzky J, Kopajtich R, Barr FA (2002) The Rab6 GTPase regulates recruitment of the dynactin complex to Golgi membranes. *Curr Biol* **12:** 1792–1795

Stenmark H (2009) Rab GTPases as coordinators of vesicle traffic. *Nat Rev Mol Cell Biol* **10:** 513–525

Stinchcombe JC, Griffiths GM (2007) Secretory mechanisms in cell-mediated cytotoxicity. *Annu Rev Cell Dev Biol* **23:** 495–517

Swan A, Nguyen T, Suter B (1999) Drosophila Lissencephaly-1 functions with Bic-D and dynein in oocyte determination and nuclear positioning. *Nat Cell Biol* **1:** 444–449

Wang X, Schwarz TL (2009) The mechanism of Ca2 + -dependent regulation of kinesin-mediated mitochondrial motility. *Cell* **136:** 163–174

Wanschers B, van de Vorstenbosch R, Wijers M, Wieringa B, King SM, Fransen J (2008) Rab6 family proteins interact with the dynein light chain protein DYNLRB1. *Cell Motil Cytoskeleton* **65:** 183–196

Wanschers BF, van de Vorstenbosch R, Schlager MA, Splinter D, Akhmanova A, Hoogenraad CC, Wieringa B, Fransen JA (2007) A role for the Rab6B Bicaudal-D1 interaction in retrograde transport in neuronal cells. *Exp Cell Res* **313:** 3408–3420

Welte MA (2004) Bidirectional transport along microtubules. *Curr Biol* **14:** R525–R537

Zahn TR, Angleson JK, MacMorris MA, Domke E, Hutton JF, Schwartz C, Hutton JC (2004) Dense core vesicle dynamics in Caenorhabditis elegans neurons and the role of kinesin UNC-104. *Traffic* **5:** 544–559

Zakharenko S, Popov S (1998) Dynamics of axonal microtubules regulate the topology of new membrane insertion into the growing neurites. *J Cell Biol* **143:** 1077–1086

Zerial M, McBride H (2001) Rab proteins as membrane organizers. *Nat Rev Mol Cell Biol* **2:** 107–117